IMPACT OF POLYMER ARCHITECTURE ON PCL-DA/PLLA SEMI-IPN PROPERTIES

An Undergraduate Research Scholars Thesis

by

KELLY G. MCKINZEY

Submitted to the Undergraduate Research Scholars program at
Texas A&M University
in partial fulfillment of the requirements for the designation as an

UNDERGRADUATE RESEARCH SCHOLAR

Approved by Research Advisor: Dr. Melissa A. Grunlan

May 2019

Major: Biomedical Engineering

TABLE OF CONTENTS

ABSTRACT

Impact of Polymer Architecture on PCL-DA/PLLA Semi-IPN Properties

Kelly G. McKinzey
Department of Biomedical Engineering
Texas A&M University

Research Advisor: Dr. Melissa A. Grunlan
Dept. of Biomedical Engineering, Dept. of Materials Science, Dept. of Chemistry
Texas A&M University

Cranio-maxillofacial (CMF) bone defects are most commonly treated with autografts despite their many limitations. Namely, the rigid autografts are difficult to shape and fit into complex defect geometries, resulting in poor osseointegration and healing. To address this issue, the Grunlan group has proposed a "self-fitting" CMF bone tissue scaffold based on a thermoresponsive shape memory polymer (SMP). Upon exposure to warm saline (T>55°C), the SMP scaffold becomes malleable and can be easily press-fitted into complex shaped defects. The SMP scaffolds are based on a linear poly(ε-caprolactone) diacrylate (PCL-DA) network, where interconnected pores are introduced via solvent casting particulate leaching (SCPL) fabrication. Recently, linear poly(L-lactic acid) (PLLA) was incorporated into the PCL-DA network as a semi-interpenetrating network (semi-IPN), and was shown to both enhance modulus and to accelerate degradation toward matching the rate of bone neotissue formation. The PCL-DA:PLLA semi-IPN's unique properties were thought to be linked to phase separation, or polymer miscibility. Since star polymers are known to have different hydrodynamic volumes and interactions than their linear counterparts, the aim of this work explored the effects of changing from a linear to star architecture in a semi-IPN. Star substitution into nonporous films yielded further tunable

properties, particularly in terms of accelerated degradation profiles, as well as mechanical and shape memory characteristics, with polymer miscibility as a main contributor.

ACKNOWLEDGEMENTS

I would like to thank Dr. Melissa Grunlan and Michaela Pfau for their guidance and support throughout the course of this research. Their constant mentorship and advice have helped spark my interest and motivation for research in biomedical engineering.

Additionally, I would like to thank my friends and family for constantly supporting my efforts and helping to achieve my goals. Finally, I would like to thank the LAUNCH program for allowing me this opportunity to further my research experience.

CHAPTER I

INTRODUCTION

Autographs are still considered the "gold standard" for treatment of cranio-maxillofacial (CMF) bone defects, despite their many limitations such as donor tissue availability, donor site morbidity, and primarily, the difficulty in shaping rigid autografts to fit tightly within the defect site.[1] This work will focus on a promising regenerative, tissue engineering strategy aimed at restoring native tissue and function via a "self-fitting" thermoresponsive shape memory polymer (SMP) scaffold to guide and support CMF bone healing.[2] The scaffolds are based on a thermoset poly(ε-caprolactone) diacrylate (PCL-DA) [linear, M_n = 10 kg/mol] network where covalent cross-links are responsible for the permanent shape, and PCL crystalline lamellae are responsible for the temporary shape. Upon heating above T_{trans} ($T_{m,PCL}$=55°C), the PCL lamellae melt allowing the material to become deformable and to be easily press-fitted into the defect site. Upon cooling to body temperature (T~37°C), the material returns to its rigid state and locks into the precise shape of the defect. This ensures a tight fit between the implant and the defect site, which is essential for osseointegration and improved healing. Solvent casting particulate leaching (SCPL) can be implemented to produce a porous PCL-DA scaffold where pore size can be tuned to promote osteoinductivity. These scaffolds are similar to bone in that they have an ideal pore size of ~200 μm, high porosity (~70%), and highly interconnected pores.[2] The interconnected porous structure facilitates bone tissue engineering by allowing the introduction of mesenchymal cells, osteotropic agents, or vasculature into the pores.[13] The PCL-DA scaffolds were previously shown to be mechanically robust with strength of ~20 MPa,[2] without being brittle like ceramic-based

alternatives, which is essential for preventing post-surgical fracture. Shape memory properties were reported with a high shape fixity (~95%) and recovery (~100%).[14]

Thermoplastic poly(L-lactic acid) (PLLA) [linear, M_n = 15 kg/mol] was incorporated into the PCL-DA network as a semi-interpenetrating network (semi-IPN). Notably, the PCL-DA/PLLA semi-IPN scaffolds were shown to have accelerated degradation profiles, with well-maintained mechanical and SMP properties.[2] PCL-DA:PLLA weight percent was systematically varied, and the 75:25 (PCL-DA:PLLA) composition showed the best mechanical properties and an accelerated degradation profile compared to the PCL-DA control.[2,10] Moving forward in this work, the wt % ratios will be maintained at 75:25 thermoset PCL:thermoplastic PLLA. PCL only constructs have been shown to degrade too slow for optimal bone healing, as PCL degrades over the course of ~1-2 years *in vivo*[3] while bone only takes ~3-12 weeks to remodel.[4] Therefore, the uniquely accelerated degradation of PCL-DA/PLLA constructs are of interest and warrant further investigation.[1]

Polymer miscibility was suspected to play a significant role in enhancing hydrolysis rates for the PCL-DA:PLLA semi-IPNs versus the PCL-DA network control.[10] Semi-IPNs and their characteristics are not well established in literature; however, blends of PCL and PLLA have reported to show phase separation that directly corresponded to faster hydrolysis rates.[15] Since scaffold approaches based on a combination of PCL and PLLA have been limited largely due to blending and copolymerization,[2] there is motivation to further explore the role of polymer miscibility in unique degradation trends observed in PCL/PLLA semi-IPNs. Thus far, the previously investigated PCL-DA:PLLA semi-IPN scaffolds have been prepared with linear polymers. Star polymers are known to have a smaller hydrodynamic radius than their linear counterparts[19], and this can affect polymer interactions (i.e. polymer miscibility) which can

potentially be used as a tool to tune degradation of PCL based semi-IPNs. This study will incorporate star polymers, of the same molecular weight (M_n), as both the thermoset and thermoplastic components of a semi-IPN to determine how polymer architecture influences scaffold properties (Figure 1).

Star polymers have previously been of interest due to their diverse thermal properties, crystallinities, and lower solution viscosity which is known to allow for improved fabrication.[5,18,19] Their incorporation into the scaffold could be used to affect the scaffolds SMP properties (based on PCL % crystallinity) and the scaffold's T_{trans} (based on PCL's T_m).[5] When polymer architecture was previously changed from linear to star in nonporous polymer films, the resulting materials were shown to degrade more quickly and have improved mechanical properties.[6,7,16] Polymer chain architecture has been shown to affect the phase behavior of materials, and star/star blends were previously found to be more miscible than linear/linear ones.[8] Due to their unique properties, incorporating polymers with star architecture into the PCL-DA/PLLA semi-IPN is expected to yield increased tunability of essential scaffold properties with polymer miscibility playing a key role.

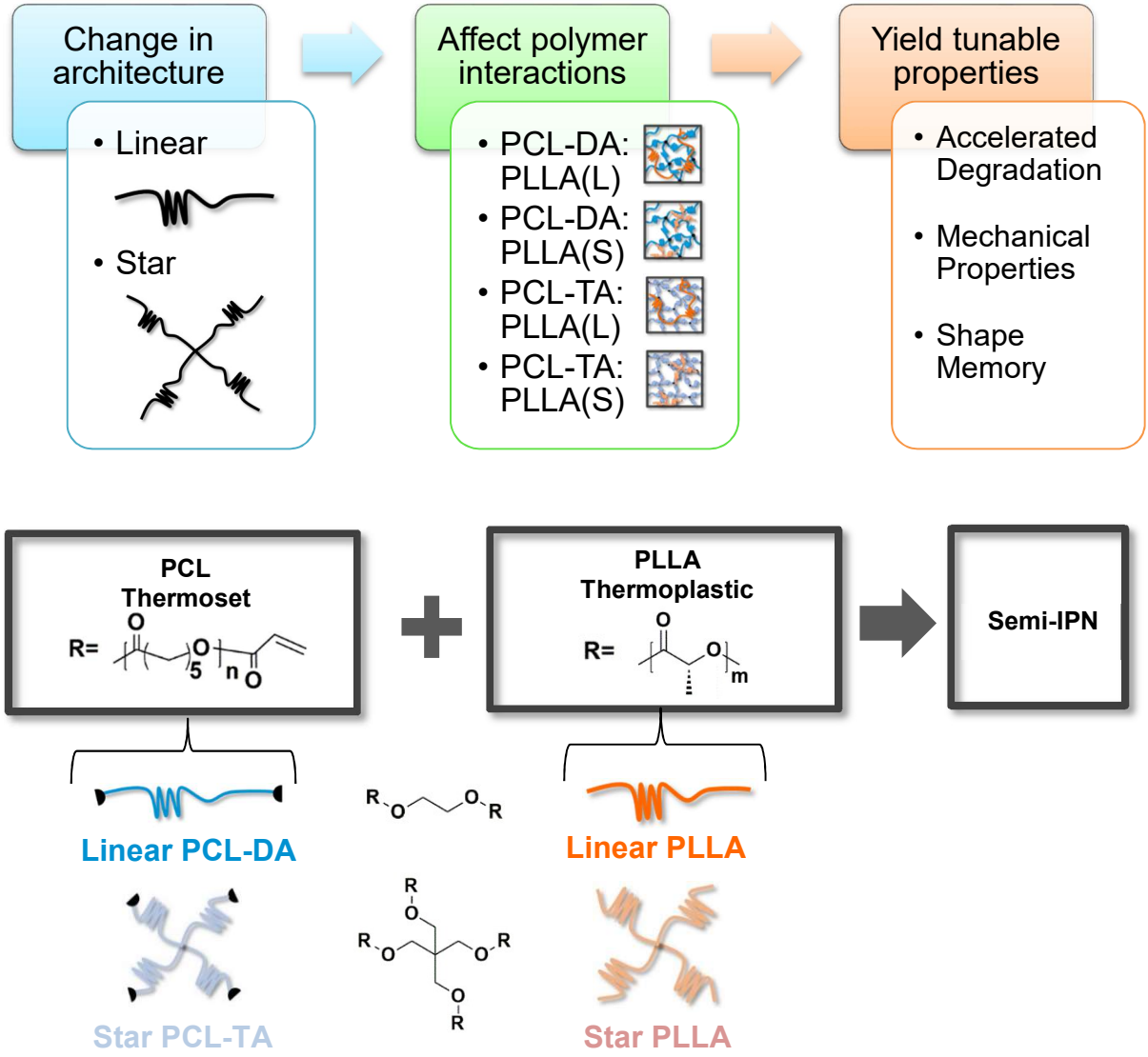

Figure 1. Summary of project.

CHAPTER II

MATERIALS AND METHODS

Materials

Polycaprolactone diol (M_n ~ 10,000 g/mol), ε-caprolactone, (3S,6S)-3,6-dimethyl-1,4-dioxane-2,5-dione (L-lactide), stannous 2-ethylhexanoate, pentaerythritol, triethylamine (Et_3N), acryloyl chloride, 4-dimethylaminopyridine (DMAP), 2,2-dimethoxy-2-phenylacetophenone (DMP), 1-vinyl-2-pyrrolidinone (NVP), potassium carbonate (K_2CO_3), sodium hydroxide (NaOH), ethylene glycol, anhydrous magnesium sulfate ($MgSO_4$), and solvents were purchased from Sigma-Aldrich. Reagent-grade dichloromethane (DCM) and NMR-grade deuterated chloroform ($CDCl_3$) were dried over 4 Å molecular sieves before use. Linear PCL-diol was purchased from Sigma-Aldrich.

Polymer Synthesis

A 4-arm star PCL-tetrol was synthesized via ring-opening polymerization (ROP) of ε-caprolactone with a pentaerythritol initiator, using stannous 2-ethylhexanoate as the catalyst.[20] Polymer molecular weight (M_n) was controlled via initiator to monomer ratio to prepare 4-arm star PCL-tetrol (10 kg/mol and 40 kg/mol) (Figure 2). A M_n of 10 kg/mol was chosen to have the overall polymer equal to the linear control, while the M_n of 40 kg/mol was chosen to have each arm equal to the M_n of the total linear control. The resulting terminal hydroxyl groups were then changed to photosensitive acrylate (OAc) groups for both the 4-arm star PCL-tetrol and the linear PCL-diol via an end group functionalization reaction with acryloyl chloride. Linear and star PLLA were synthesized via a ROP of L-lactide with ethylene glycol or pentaerythritol respectively as the

initiator, and stannous 2-ethylhexanoate as the catalyst. Target M_n and acrylate functional groups were confirmed by proton nuclear magnetic resonance (^{1}H NMR).

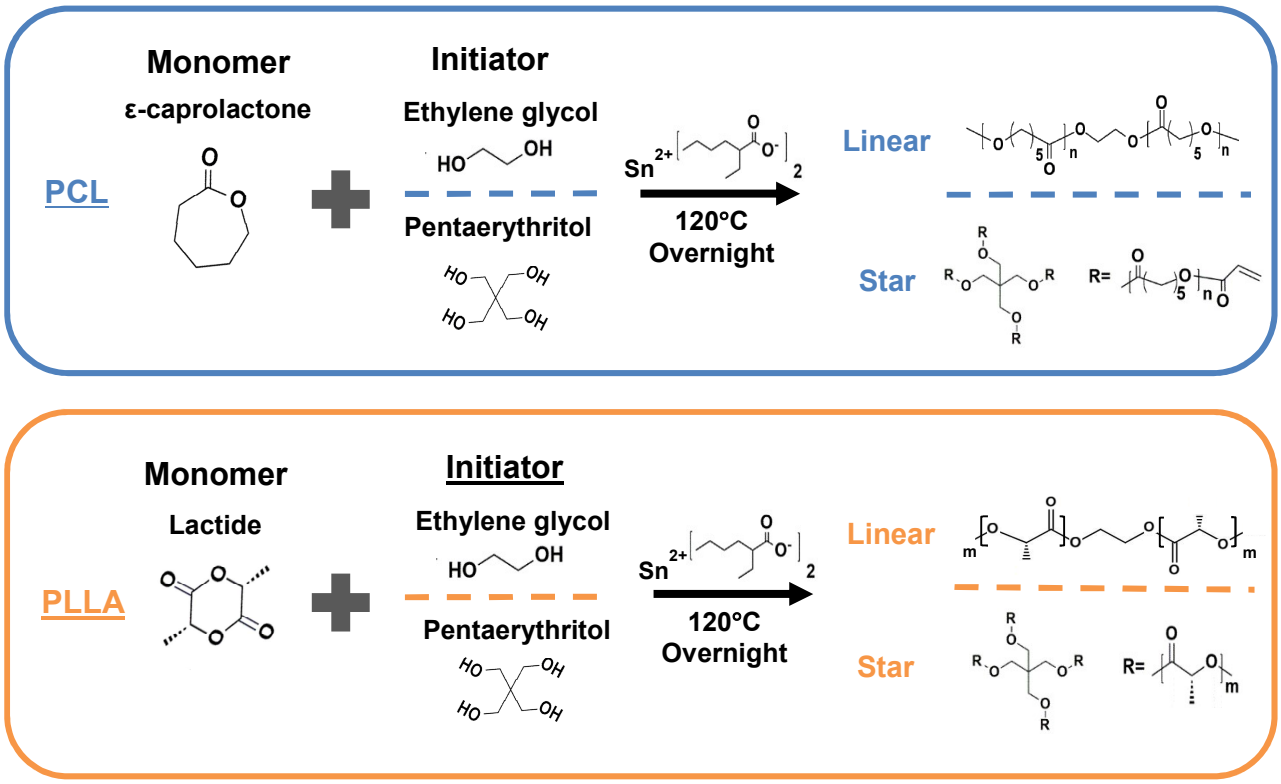

Figure 2. Schematic of polymer synthesis.

Fabrication

Three PCL controls: 10k PCL-DA, 10k PCL-TA, and 40k PCL-TA were prepared as 100% PCL networks. The 40k PCL-TA was not used in semi-IPNs because of difficulties in acrylation reactions with low % yield. Four 75:25 PCL-OAc:PLLA semi-IPNs were prepared with each of the different possible polymer architecture combinations [PCL-DA:PLLA(L), PCL-DA:PLLA(S), PCL-TA:PLLA(L), PCL-TA:PLLA(S)]. These six compositions (10k linear and star controls, 4 semi-IPNs) were fabricated into solid films using macromer solutions (25 wt% of total polymer in DCM) with 15 vol% of photoinitiator solution (10 wt% DMP in NVP). The macromer solution was transferred to a circular silicone mold (45 mm x 2 mm; McMaster-Carr) secured between glass

slides and exposed to UV light (UV-Transilluminator, 6 mW cm^{-2}, 365 nm) for 3 min per side. The solvent swollen disk was sequentially removed from the mold, air dried (RT, 12 h), dried in vacuo (36 in.Hg, RT, 4 h), soaked in ethanol (3 h), and air dried. The film was finally annealed (36 in.Hg 85 ºC, 1 h) and allowed to set at RT (48 h) before testing (Figure 3).

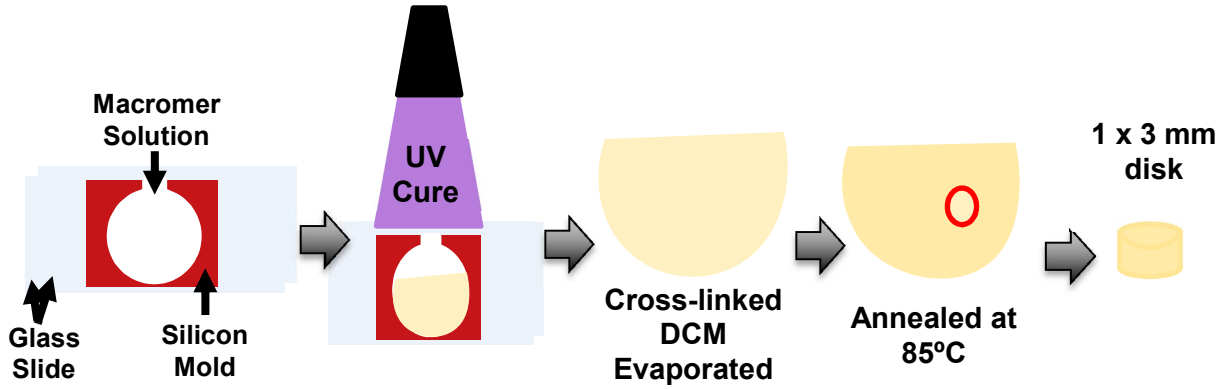

Figure 3. Schematic of film fabrication procedure.

Characterization

Polymer Only Characterization

^{1}H NMR was conducted on polymer solutions (~15 mg/ 0.7 mL) in deuterated chloroform ($CDCL_3$) using 400 MHz Inova NMR spectrometer (n = 64). Results were analyzed to confirm polymer M_n and end group functionalization success.

Differential scanning calorimetry (DSC, TA Instruments Q100) was performed (~10mg; N = 3) in hermetic pans at a heating rate of 5 ºC min^{-1} for two cycles. PCL samples were run from -100 ºC to 100 ºC, and samples of PLLA were run from 0 ºC to 180 ºC. From the endothermic PCL or PLLA melting peaks from the second cycles, melting temperature (T_m) and enthalpy change (ΔH_m) were measured. Percent crystallinity (% χ_c) was calculated via Equation (1)

$$\% \chi_c = \frac{\Delta H_m}{\Delta H^\circ_m} \text{ x } 100, \quad (1)$$

where ΔH_m was calculated by the area of the melting peak, and ΔH°_m is the enthalpy of fusion of 100% crystalline PCL (139.5 J g^{-1}) or PLLA (93.0 J g^{-1}).[9]

Polarizing Optical Microscopy (POM) images were acquired using a Zeiss Axiophot equipped with a polarizer to visually compare the spherulite sizes of the PCL polymers of both star and linear architecture. ImageJ software was used to quantitatively determine the average spherulite size.

Semi-IPN Composition

Thermogravimetric analysis (TGA, TA Instruments Q50) of specimens (~10 mg, N = 1) in platinum pans was run under N_2 from RT to 500 ºC at a heating rate of 10 ºC min^{-1}. The mass of the samples throughout heating was measured to quantify percent mass remaining. This allows for verification the target PCL-DA:PLLA ratio of 75:25 or 100:0 since the thermoplastic PLLA thermally degrades at ~280 ºC while the thermoset PCL degrades at ~500 ºC.

Discs (~7 mm x ~1.1 mm; N = 3) were immersed in 10 mL DCM and maintained for 48 hr at 150 rpm. Swollen discs were removed, air dried, and dried in vacuo (36 in.Hg, RT, ~16 h). The mass of dried discs was determined to quantify percent mass loss (i.e. sol content). A low sol content (< 12% of cross-linked polymer) confirmed the PCL-OAc network was effectively crosslinked. In semi-IPNs, thermoplastic, non-crosslinked PLLA was also extracted, so a sol content of <37% (~25% PLLA + <12% PCL-DA) confirmed the semi-IPN network was effectively crosslinked. Disks of the same size were immersed in 10 mL DCM for 1 hr at 150 rpm. Swollen disks were removed, and change in volume was measured by monitoring thickness and diameter of the swollen disks to determine relative cross-link density.

Thermal Properties

DSC of film specimens (~10mg; N = 3) in hermetic pans was run from RT to 100 ºC at the same rate as polymer only DSC. Both T_m and ΔH_m were measured, and % χ_c was calculated with a wt% correction via Equation (2)

$$\% \chi_c = \frac{\Delta H_m}{\Delta H°_m * w} * 100 \quad (2)$$

where *w* is the weight fraction of polymer in the film (i.e. $w_{PCL} = 0.75$ or $w_{PLLA} = 0.25$).

Shape Memory Behavior

Rectangular specimens (~20 mm x ~3.3 mm x ~1.1 mm) were subjected to the following sequence: (1) after exposure to a water bath at ~80 ºC ($T>T_{trans}$) for 1 min, the film strip was deformed into a coiled shape with a metal mandrel, (2) the film was placed in an ice bath (~0 ºC, $T<T_{trans}$) for 1 min to fix the temporary shape, (3) the fixed coil was placed in the 80 ºC water bath and recovery was observed at t = 0 and 8 s.

Mechanical Properties

Tensile properties of films were evaluated at RT with a tensile tester (Instron 5594) by subjecting rectangular strips (~15 mm x ~3.3 mm x ~1.1mm; N = 8) with a gauge length of ~3 mm to a constant strain rate (50 mm min^{-1}) in tension until break. From the resulting stress-strain curves, modulus (E), tensile strength (TS), and strain at break (% ε) were determined.

Accelerated Degradation

Disks (~7 mm x ~1.1 mm; N = 3) punched from the solid SMP films were immersed in 10 mL of 1 M NaOH in glass vials maintained at 37 ºC by use of an incubator shaking at 60 rpm. Testing parameters for *in vitro* degradation outlined in ASTM F1635 for surgical implants were

followed.[11] Samples were taken out at 8, 24, 48, 72, and 168 h; they were thoroughly rinsed with DI water, blotted, and dried in vacuo (36 in.Hg, RT, ~16 h). Gravimetric analysis was performed, and the percent mass loss was determined. At ~15% and ~50% mass loss, samples were imaged via scanning electron microscopy (SEM). Surfaces and cross sections were subjected to Au-Pt coating (≈4 nm). Images were obtained using a JOEL 6400 SEM with an accelerating voltage of 10 kV.

Phase Separation

Non-degraded samples were visualized via SEM to qualitatively examine phase separation, or polymer miscibility, of the film compositions. Surfaces were subjected to Au-Pt coating (≈4 nm). Images were obtained using a Tescan Vega SEM with an accelerating voltage of 10 kV.

Statistical Analysis

Data was reported as the mean ± standard deviation. Values were compared using the Holm-Sidak method to determine *p*-values.

CHAPTER III

RESULTS

Polymers

PCL

Two star polymers were prepared based on the previously studied linear 10 kg/mol PCL-diol: PCL-tetrol with M_n = 10 kg/mol (total comparable to linear) and PCL-tetrol with M_n = 40 kg/mol (each arm had the same M_n as the linear). PCL polymer structure, M_n and functionalization with acrylate end groups was verified via ^{1}H NMR (Appendix Figure A1).

POM imaging was also used to verify M_n of 10k PCL-diol versus 10k PCL-tetrol (Figure 4a and Figure 4b). The 40k PCL-tetrol was not verified via POM because of the difference in M_n; this change in M_n would show inconclusive results as it is unknown how the 40k spherulites should compare to the 10k spherulites. The average area of PCL-diol spherulites was 17.3 ± 5.53 mm, while the average area of PCL-tetrol spherulites was 1.11 ± 0.176 mm. While both polymers have the same total M_n, a 4 arm star polymer would have a shorter M_n of each arm compared to a linear polymer; therefore, the smaller spherulite size of the 10k PCL-tetrol verifies a star architecture.

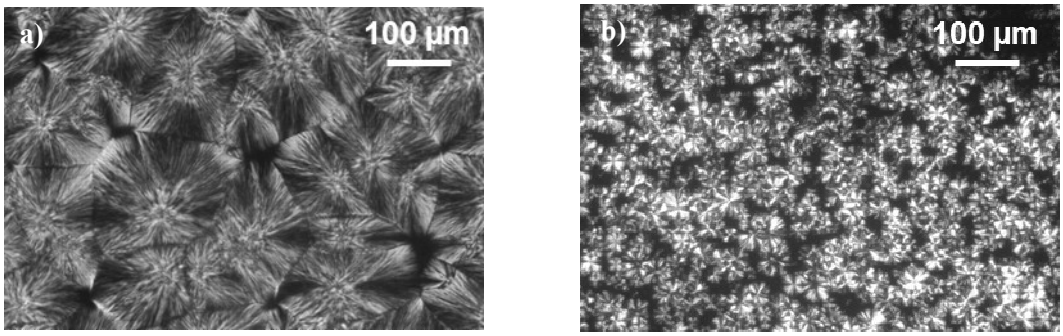

Figure 4. a) 10k PCL-diol POM image & b) 10k PCL-tetrol POM image.

DSC was used to determine T_g, T_m, and % crystallinity of the PCL-tetrols compared to the PCL-diol control (Table 1 and Appendix Figure A2). The 10k PCL-tetrol had a lower T_m of 49.9 ± 0.40 ºC compared to the 10k PCL-diol of 52.6 ± 0.16 ºC. The PCL % Crystallinity was higher for the 10k and 40k PCL-tetrols (55.2 ± 2.1% and 53.0%) compared to the 10k PCL-diol (46.5 ± 0.20%). The T_g of all three PCLs was approximately -64 ºC.

Table 1. DSC characterization of various PCLs.

Polymer	T_g (ºC)	T_m (ºC)	% Crystallinity
10k PCL-diol	-65.2 ± 0.98	52.6 ± 0.16	46.5 ± 0.20
10k PCL-tetrol	-63.3 ± 1.2	49.9 ± 0.40	55.2 ± 2.1
40k PCL-tetrol*	-63.8	54.2	53.0

*Composition was not run in triplicate

Thermoplastic PLLA

In previous work, linear PLLA with M_n =15 kg/mol greatly enhanced the degradative and mechanical properties of PCL-DA films and scaffolds.[2] The total M_n was held constant for both the linear and star PLLA synthesized herein. PLLA structure and target M_n was verified by ^{1}H NMR (Appendix Figure A3). DSC was used to determine T_g, T_m, and % crystallinity of the star PLLA compared to the linear PLLA (Table 2 and Appendix Figure A4). Star PLLA had a higher T_m (+ 3.0 ºC) and % crystallinity (+ 2.9 %) than linear PLLA.

Table 2. DSC characterization of PLLA thermoplastics.

Polymer	T_g (ºC)	T_m (ºC)	% Crystallinity
Linear PLLA ~15k	45.1 ± 0.72	155 ± 0.35	52.8 ± 0.14
Star PLLA ~15k	48.2 ± 2.7	158 ± 2.5	55.7 ± 12

Films

PCL-OAc Thermal Properties

Films were made starting with the different M_n PCL-OAcs to ensure adequate cross-linking occurred before adding the thermoplastic PLLA component. The 10k PCL-DA, 10k PCL-TA, and

40k PCL-TA films were created as PCL only controls. PCL-OAc T_m and % crystallinity were determined for the three networks, all showing a decrease of % crystallinity yet maintaining their respective T_m after being crosslinked. The 10k PCL-TA showed a significantly lower ($p<0.05$) crystallinity (16.7 ± 4.1) than the 10k PCL-DA (39.6 ± 1.1), while the 40k PCL-TA (43.7 ± 0.58) was significantly higher than PCL-DA (Figure 5a). This could be due to the short arms of the 10k star PCL-TA, so the PCL chains between crosslinks are less able to organize into lamellae.

PCL-OAc Crosslinking

Sol content confirmed that the 10k PCL-DA and 10k PCL-TA networks were effectively crosslinked because the % mass loss was 10.9 ± 1.6 and 5.09 ± 1.3, respectively. However, the 40k PCL-TA % mass loss was 29.8 ± 1.4; this is significantly higher than the acceptable 12% and the 40k PCL-TA film was compromised due to lack of cross-linking (Figure 5b). To show the relative crosslink density, the % increase in thickness and diameter from the original shape, or swelling, was determined (Figure 5c). The 10k PCL-TA had the lowest % swelling of 82.1 ± 9.9 and, therefore, the highest crosslink density. The 40k PCL-TA % swelling of 129 ± 16 showed that it had the lowest crosslink density, and the 10k PCL-DA had a % swelling of 109 ± 2.3, showing a medium crosslink density. These results were expected, as crosslink density is based on the length of polymer chains between cross-links. This is reasonable because the 10k PCL-TA has 5k long chains, 10k PCL-DA has 10k chains, and 40k PCK-TA has 20k chains, thus demonstrating the highest, medium, and lowest crosslink densities, respectively.

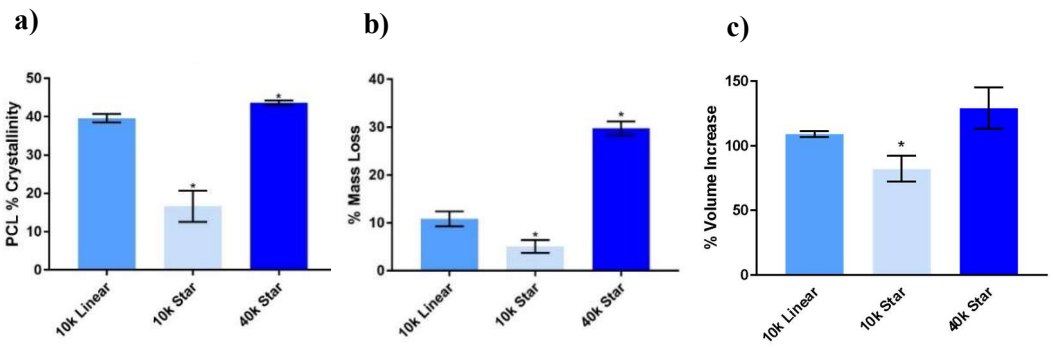

Figure 5. a) PCL % Crystallinity, b) Sol Content, & c) Swelling.

PCL-OAc Mechanical Properties

The tensile modulus (E), and tensile strength (TS) were recorded on the three control PCL-OAc films, and both PCL-TA films were significantly different compared to the PCL-DA control (Appendix Figure A5). Moving forward with semi-IPNs, the 10k PCL-DA and 10k PCL-TA was used for controls as well as the thermoset component of PCL/PLLA semi-IPNs. The 40k PCL-TA was not used due to a high sol content value showing the 40k PCL-TA did not undergo adequate cross-linking. It was also observed that the 40k PCL-tetrol was challenging to synthesize and acrylate due to high viscosity. The % yield of 10k PCL-DA was ~75%, 10k PCL-TA was 74%, and 40k PCL-TA was a mere 36%; therefore, the 40k PCL-TA was not used to prepare the semi-IPNs.

Semi-IPN Composition

To verify the semi-IPN PCL-OAc:PLLA wt% ratio, TGA was used. Thermoplastic PLLA underwent degradation at a distinguishably lower temperature (~280 ºC) than the PCL-OAc network, so the wt% of each of PCL-OAc and PLLA in the semi-IPN could be determined by looking at the % mass loss at that temperature. Mass loss of ~25% of all four semi-IPNs occurred at the ~280 ºC temperature, while the controls showed 0% mass loss at that temperature, as expected based on the target weight ratios (Figure 6a and Figure 6b). Next, sol content confirmed

that the PCL-DA and PCL-TA controls were effectively crosslinked, with a % mass loss of 11.9 ± 0.72 and 11.2 ± 1.4, respectively. In semi-IPNs, thermoplastic, non-crosslinked PLLA was also extracted so a sol content less than ~37% (~25% PLLA + <12% PCL-DA) confirmed the four semi-IPN networks were effectively crosslinked. Hence, due to the high degree of acrylation, PCL-OAc was able to successfully cross-link in the presence of PLLA, and no composition reached the threshold maximum of 37% (dashed line on Figure 6c) mass loss to prove otherwise (Figure 6c).

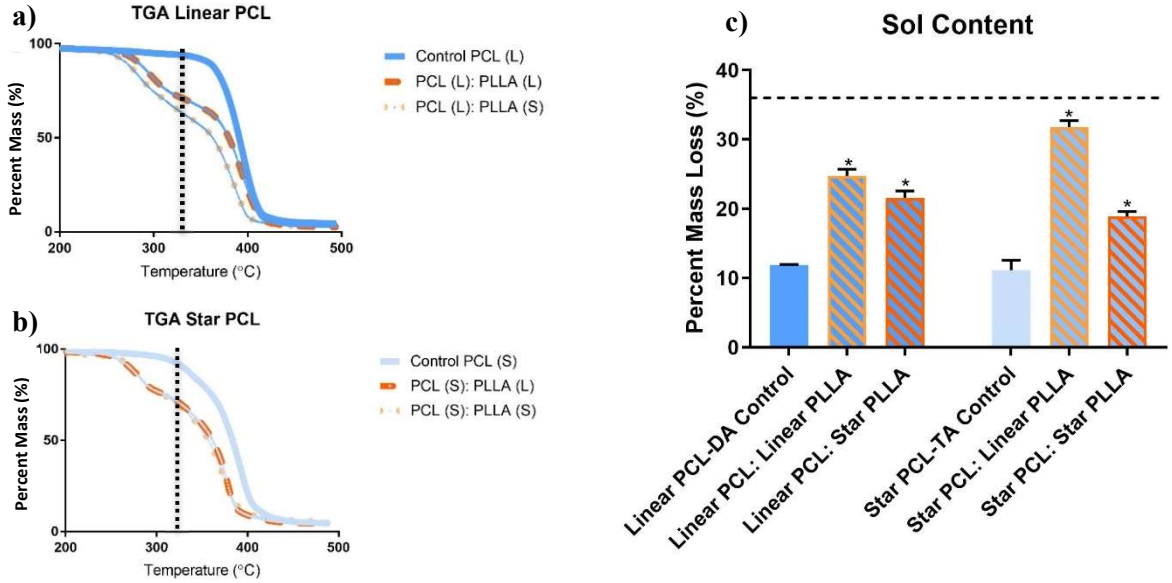

Figure 6. a) TGA of PCL-DA control and semi-IPNs b) TGA of PCL-TA control and semi-IPNs & c) Sol content of the six compositions.

Semi-IPN Thermal Properties

T_m and % crystallinity for both PCL and PLLA components were determined for all networks (Figure 7a and Figure 7b). Prior to incorporation into films, PCL showed ~51.6% crystallinity, while PLLA showed ~54.3% crystallinity. When crosslinked, all compositions had a significantly lower PCL % crystallinity. Interestingly, the PCL-DA compositions were reduced to 39% PCL crystallinity, while the PCL-TA compositions were even further reduced to ~29% PCL crystallinity. The PLLA % crystallinity also showed significantly lower values after crosslinking in all semi-IPN compositions. Linear PLLA compositions with PCL-DA and PCL-TA had PLLA

% crystallinities of 48.6 ± 0.45 and 42.2 ± 0.29 respectively. Star PLLA compositions with PCL-DA and PCL-TA had % crystallinities of 39.7 ± 0.14 and 30.8 ± 0.23, showing a significantly lower PLLA % crystallinities compared to the linear PLLA compositions. All polymers showed restricted crystallinity after incorporation into films, and star PCL & PLLA were more restricted than their linear counterparts.

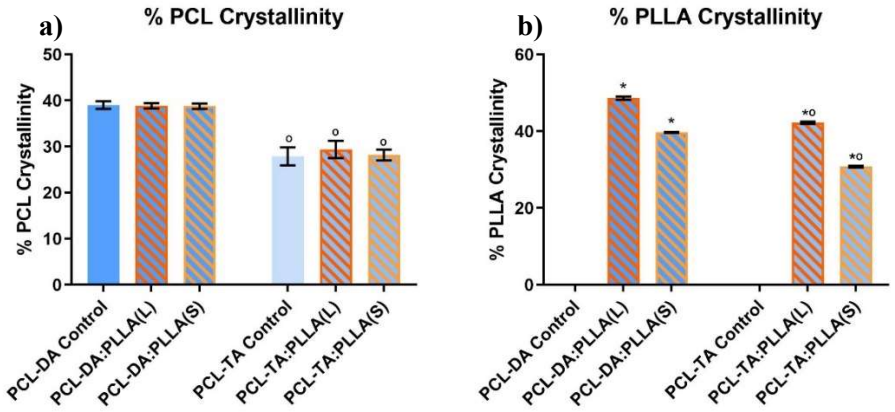

Figure 7. a) % PCL Crystallinity & b) % PLLA Crystallinity for all six compositions.

Semi-IPN Accelerated Degradation

Degradation behavior was assessed under accelerated conditions (1 M NaOH, 37 ºC, 60 rpm) in terms of quantitative mass loss and qualitative surface morphology analysis. Mass loss occurred at a substantially faster rate for PCL-OAc:PLLA semi-IPNs versus the corresponding PCL-OAc network controls, which showed effectively negligible weight loss over the span of 1 week (Figure 8a and Appendix Figure A6). For semi-IPNs comprised of linear PLLA, there was a rapid increase in mass loss compared to semi-IPNs with star PLLA. We hypothesize that phase separation may play more of a role rather than crystallinity since compositions with linear PLLA had an increase in mass loss but had higher % crystallinity. The higher % crystallinity would typically mean a slower degradation rate, but this is not the case suggesting that polymer interactions or miscibility may play a key role instead. All the semi-IPNs had a significantly faster

degradation profile compared to the PCL-OAc controls. The impact of star architecture showed different degradation rates, i.e. tunability, dependent upon which architecture of thermoplastic PLLA was used in the semi-IPN. All films were visualized at both ~15 % and ~50 % mass loss under SEM (Figure 8b and Figure 8c). ATR-FTIR was performed on the films before degradation to quantify relative amount of PCL-OAc and PLLA at the surface. Interestingly, more PLLA was found on the surface of semi-IPNs with linear PLLA, and this may lend insight since linear PLLA semi-IPNs degraded the most quickly (Appendix Figure A7).

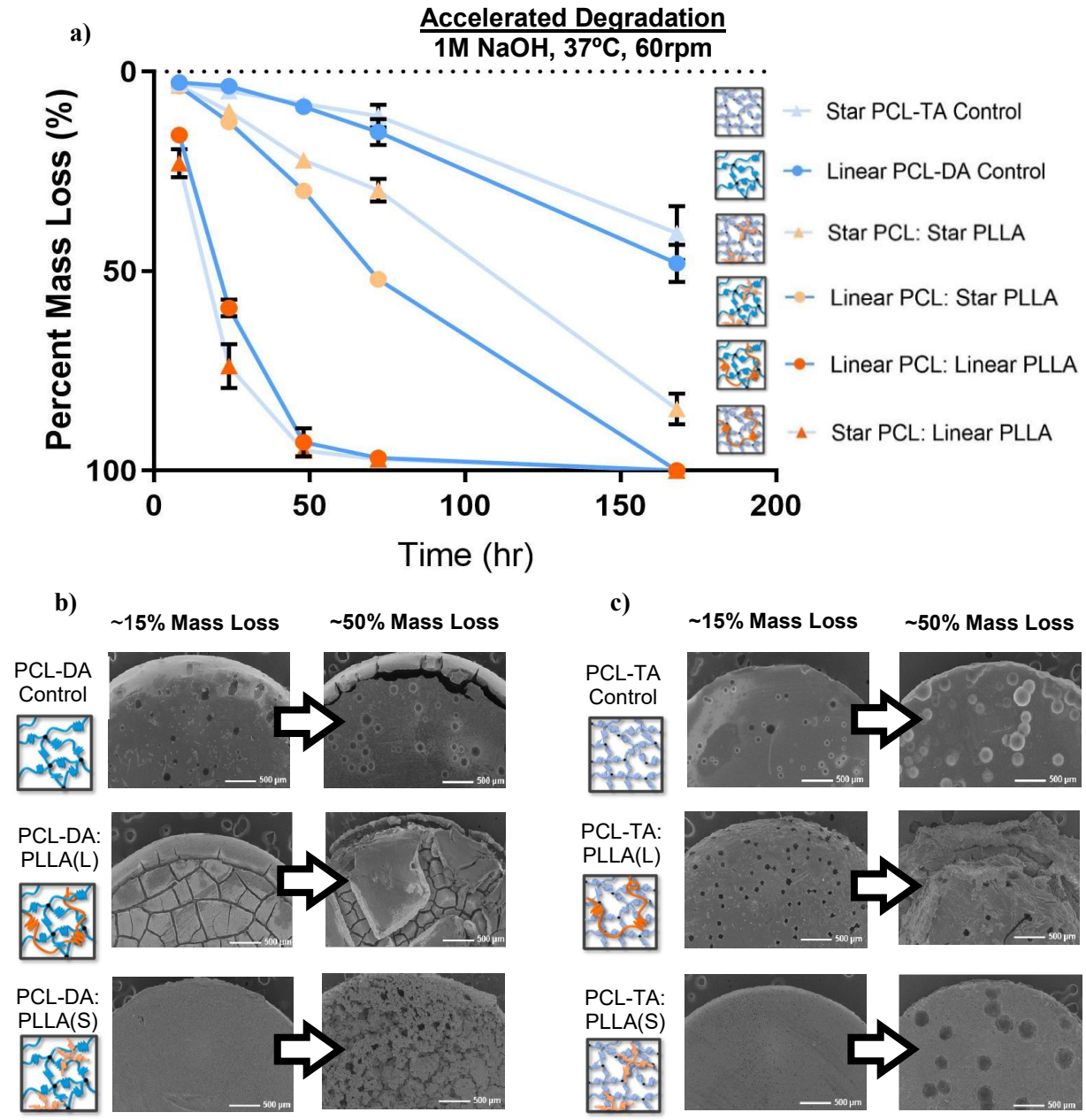

Figure 8. a) Accelerated degradation, b) SEM of PCL-DA compositions at ~15% and ~50% mass loss, & c) SEM of PCL-TA compositions at ~15% and ~50% mass loss.

Semi-IPN Phase Separation/Miscibility

SEM images of non-degraded films were acquired to observe polymer miscibility, or phase separation. Literature shows differences in miscibility between star and linear blends,[8] and our semi-IPN networks could show a unique variation of polymer miscibility. SEM images were compared, and the presence of bubble-like textures was indicative of phase separation, or polymers

coalescing and separating; films with more of this texture were ranked as less miscible. Differences in surface morphology, indicative of differences in film miscibility, were observed when comparing the films with the same PCL-OAc architecture (Figure 9). The PCL-OAc controls had smooth surfaces proving they were completely miscible. The semi-IPNs where then ranked based on a relative comparison to these PCL-OAc controls. When comparing semi-IPNs to each other, compositions with star PLLA were ranked as immiscible (covered in bubbles) compared to the linear PLLA, which appeared to be partially miscible (fewer bubbles, but still more than the controls). Interestingly, partially miscible compositions degrading the quickest, immiscible compositions slightly slower, and miscible compositions the slowest. Partially miscible networks also had the most improved mechanical properties. These trends are consistent with ongoing work in the Grunlan lab on semi-IPNs.

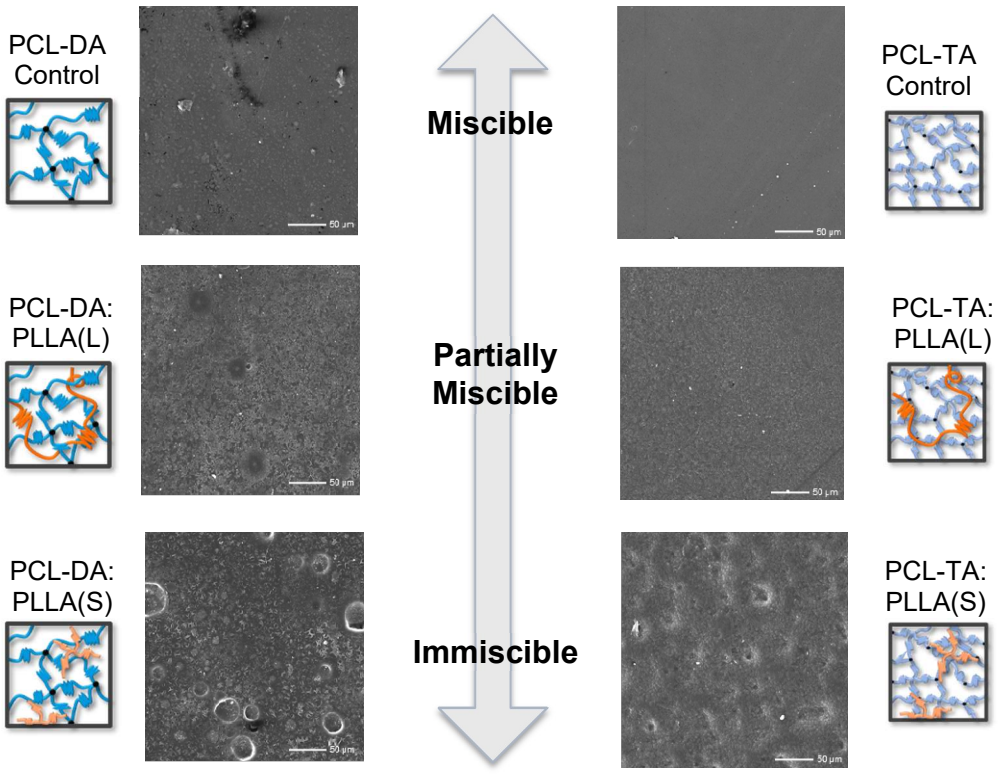

Figure 9. SEM images of non-degraded films, showing miscibility.

Semi-IPN Shape Memory Behavior

Qualitative shape fixity and recovery was observed macroscopically for all films (Figure 10). All films were placed in ~80 ºC ($T>T_{trans}$) water, wrapped around a mandrel to create a temporary shape (coil), allowed to cool, then placed back in ~80 ºC ($T>T_{trans}$) water. PCL crystalline domains maintain the temporary shape and, upon melting, dictate recovery.[10] The PCL-TA control did not display shape fixity, which is likely due to its significantly lower % crystallinity compared to PCL-DA. PCL-TA broke when trying to hold the temporary coil shape; however, the addition of the thermoplastic PLLA (star or linear) uniquely restored the shape fixity, as those compositions were observed to hold their temporary coil shape. PCL-TA was shown to have high crosslink density and reduced crystallinity in films compared to PCL-DA, so the crystalline domains may not be able to fully form thereby limiting the switching segments ability to be deformed and locked into a temporary shape. While semi-IPNs are not widely reported on, similar phenomena have been shown in double network hydrogels. Double network hydrogels consist of a brittle first network and a ductile second network; the addition of the ductile second network is known to improve hydrogel strength and toughness.[12] The addition of thermoplastic PLLA as a semi-IPN may act analogously as a second ductile component that can restore the shape memory properties of brittle PCL networks.

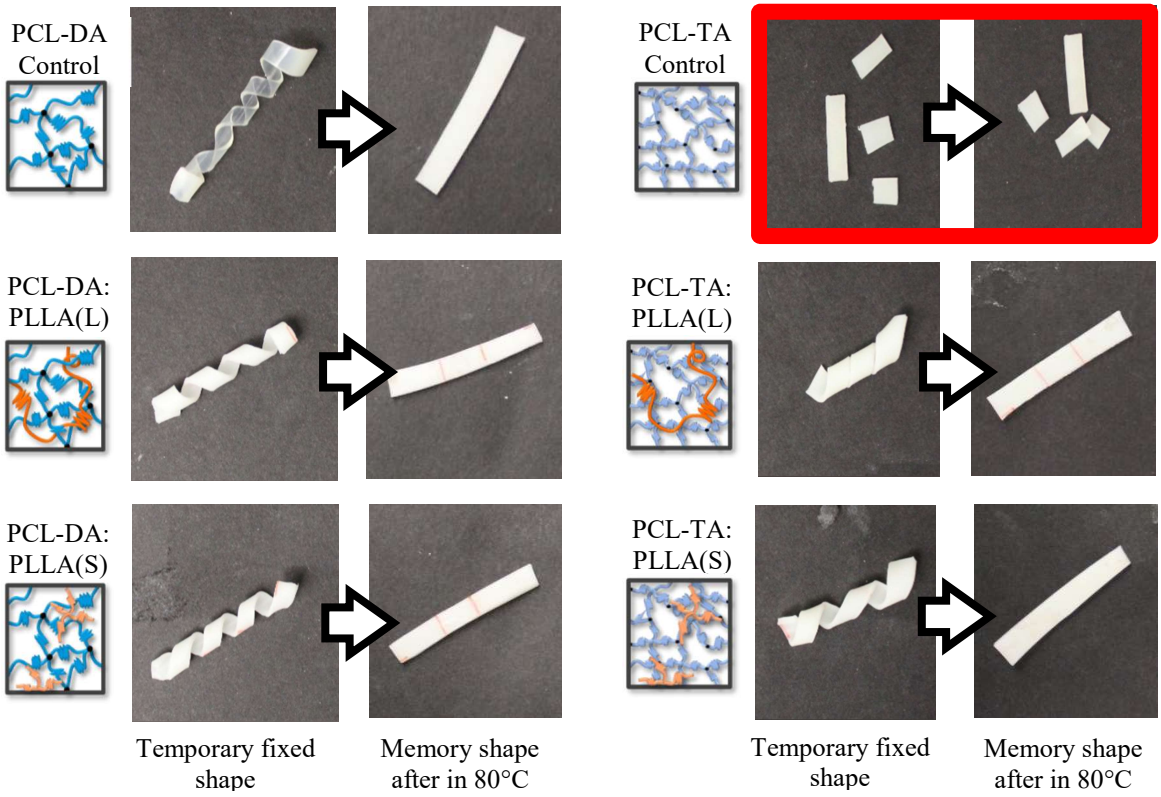

Figure 10. Shape memory properties all films.

Semi-IPN Mechanical Properties

The tensile modulus (E), and tensile strength (TS) were determined for all SMP networks (Figure 11a and Figure 11b). The PCL-DA control showed a significantly greater modulus of 134 ± 10 MPa compared to the PCL-TA control of 103 ± 9.1 MPa, but the TS was maintained at ~18.4 MPa for both. PCL-TAs modulus is likely weaker than PCL-DAs due to reduced crystallinity. For semi-IPNs, a ~50% increase in *E* was observed compared to their PCL control for both linear and star PLLA compositions. This trend of semi-IPNs having increased modulus compared to controls is consistent with previous data.[10] The PCL-DA: PLLA (L) composition had a modulus of 196 ± 9.9 MPa and TS of 21.6 ± 2.5 MPa. This *E* and TS was not significantly different than the PCL-TA: PLLA (L) counterpart having a modulus of 179 ± 23 MPa and tensile strength of 20.3 ± 2.3 MPa despite PCL-TA initially having a weaker modulus. The PCL-DA: PLLA (S) composition

had a 195 ± 11 MPa *E* and a 22.0 ± 2.0 MPa TS, which was significantly higher than the PCL-TA: PLLA (S) counterpart. This composition had the lowest *E* and TS of all semi-IPNs of 171 ± 27 MPa and 18.8 ± 3.4 MPa, respectively, but still had better mechanical properties than the PCL-TA control. With the inclusion of thermoplastic PLLA, semi-IPNs showed tunability in degradation rates, while the mechanical and SMP properties were maintained or restored compared to the PCL-OAc controls.

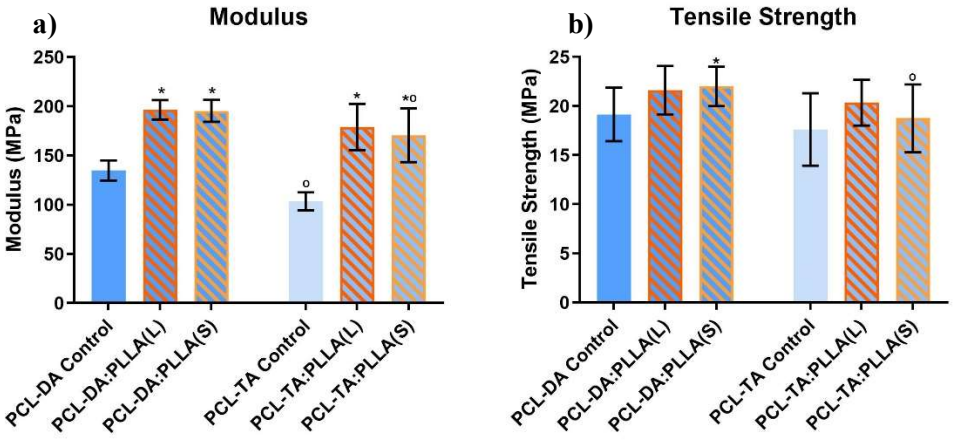

Figure 11. a) Tensile Modulus & b) Tensile Strength.

CHAPTER IV

CONCLUSION AND FUTURE WORK

Conclusion

SMP scaffold implants made up of semi-IPNs of cross-linked PCL and thermoplastic PLLA have the potential to be "fitted" within irregular CMF bone defects to promote regenerative healing, while also possessing favorable and tunable properties. In this work, nonporous films comprised of linear and star thermoset PCL-OAc with linear and star thermoplastic PLLA were prepared to assess their degradative, mechanical, and shape memory properties. Four armed PCLs of two M_n (10 kg/mol and 40 kg/mol) were successfully synthesized to compare to the control PCL-DA (M_n = 10 kg/mol). These were then turned into nonporous films to ensure adequate crosslinking occurred before adding the thermoplastic PLLA component for a semi-IPN. Compared to the PCL-DA control (39.6 ± 1.1%), the PCL % crystallinity of the 10k PCL-TA (16.7 ± 4.1%) was significantly lower, while the 40k PCL-TA (43.7 ± 0.58%) was significantly higher. Percent swelling confirmed the expected relative crosslink densities of all PCLs; however, sol content showed the 40k PCL-TA's crosslinking was compromised with a % mass loss of 29.8 ± 1.4% which was well over the acceptable amount of 12%. Because of the lack of crosslinking capability and low yield (36%) of 40k PCL-TA, only 10k PCL-DA and 10k PCL-TA were used for the thermoset in the semi-IPNs.

Two PCL controls (PCL-DA and PCL-TA) and four semi-IPNs [PCL-DA:PLLA(L), PCL-DA:PLLA(S), PCL-TA:PLLA(L), PCL-TA:PLLA(S)] of 75:25 wt% PCL-OAc:PLLA were prepared and cured into films. TGA confirmed the 75:25 PCL-OAc:PLLA wt% of all 4 semi-IPNs, and sol content verified all compositions were successfully crosslinked because the % mass loss

was less than the acceptable 37%. DSC analyses showed significant a significant reduction in both PCL and PLLA crystallinities after incorporation into a film; star PCL & PLLA were further restricted compared to their linear counterparts. Degradation profiles were obtained, and all semi-IPNs degraded at a faster rate than the PCL-OAc controls, which is improving toward the rate of bone neotissue formation. Implementing star architecture also provided more tunability in degradation than with a linear only semi-IPN. This tunability of degradation could be advantageous, as the semi-IPN scaffold could be tailored to best suit specific patient and location of bone, as bone heals differently for children than adults in various locations. SEM images provided an interesting look into polymer miscibility, which seems to play a major role in polymer degradation. Linear PLLA compositions were more miscible than the star PLLA compositions, and those linear PLLA compositions interestingly showed faster degradation profiles as well as improved mechanical properties than the PCL-OAc controls. Qualitative shape memory behavior was macroscopically observed, and all compositions except for the PCL-TA control displayed excellent shape fixity and recovery properties. The PCL-TA control broke while attempting to form its temporary shape, but the inclusion of semi-IPN thermoplastic PLLA was found to uniquely restore the SMP properties of the PCL-TA network. Additionally, the PCL-OAc:PLLA semi-IPNs have shown enhanced mechanical properties, increase of ~36% modulus, when compared to the PCL-OAc controls. With the inclusion of thermoplastic PLLA, semi-IPNs showed tunability in degradation rates toward bone healing, while maintaining robust mechanical properties and the ability to "self-fit" into complex geometries. In summary, PCL-OAc:PLLA semi-IPNs of various architectural combinations were prepared in nonporous films. These were examined for their thermal, degradative, shape memory, and mechanical properties, and the semi-IPNs displayed excellent overall properties compared to their PCL-OAc controls.

Future Work

This work was limited to films to explore nonporous SMP qualities of varying polymer architecture in semi-IPNs. Moving forward, all six compositions will be utilized in the form of porous bone tissue scaffolds. These will be fabricated via SCPL[17] shown in Figure 12. Consistent with film results, the semi-IPNs demonstrated accelerated degradation profiles and enhanced mechanical properties (i.e. *E* and TS) compared to the PCL-OAc controls in preliminary studies (Figure 13a and Figure 13b). All semi-IPNs degraded significantly faster than the PCL-OAc controls, and they all degraded at slightly different rates, proving tunability in the different architectures. At the 72 hr time point, the PCL-OAc controls degraded the slowest, with PCL-DA having a % mass loss of 25.0 ± 22 % and PCL-TA of 9.93 ± 10%. PCL-TA:PLLA(L) had the largest % mass loss of 93.9 ± 9.8%. PCL-TA:PLLA(S) had a % mass loss of 89.9 ± 16%, showing the PCL-TA semi-IPNs had the fastest degradation profiles. The PCL-DA compositions with linear and star PLLA had % mass losses of 66.3 ± 37% and 83.2 ± 20%, respectively. The modulus was also significantly improved from the PCL-OAc controls, as the PCL-DA and PCL-TA controls had compressive moduli of 9.65 ± 2.8 MPa and 3.57 ± 0.58 MPa, respectively. The PCL-DA semi-IPNs had an enhanced modulus of ~20 MPa, while the PCL-TA semi-IPNs had a modulus of ~11 MPa. Further studies will be performed on the semi-IPN scaffolds such as a larger degradation study, shape memory investigation, and pore size/interconnectivity examination. These scaffolds are expected to behave similar to their nonporous film results previously shown, in that the semi-IPNs have better and tunable degradative, mechanical, and shape memory properties than the controls.

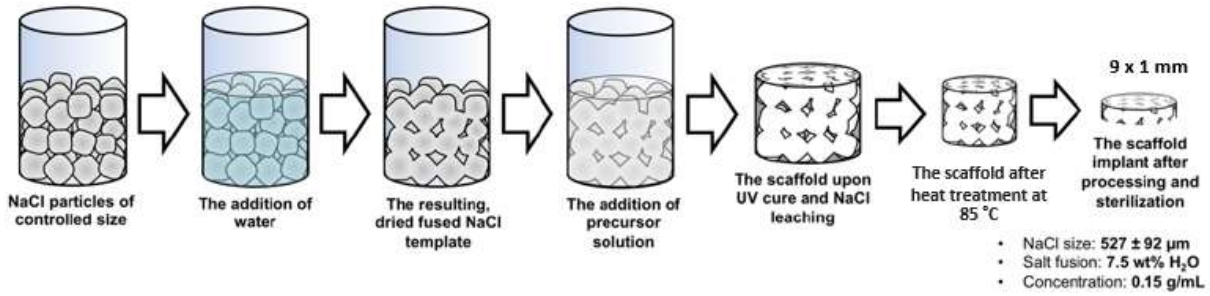

Figure 12. Schematic of SMP scaffold implant fabrication procedure.

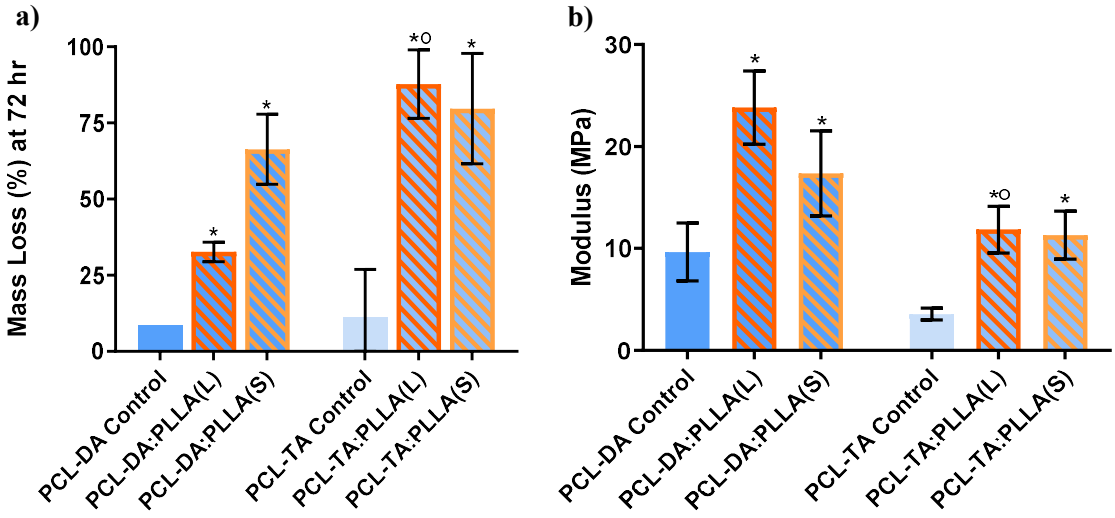

Figure 13. a) Degradation of scaffolds at 72 hours & b) Modulus of scaffolds.

REFERENCES

1 Pfau, M. P. Biodegradable Shape Memory Polymer (SMP) Scaffolds to Heal Craniomaxillofacial (CMF) Bone Defects.

2 Woodard, L. N.; Kmetz, K. T.; Roth, A. A.; Page, V. M.; Grunlan, M. A., Porous Poly(ε-caprolactone)–Poly(l-lactic acid) Semi-Interpenetrating Networks as Superior, Defect-Specific Scaffolds with Potential for Cranial Bone Defect Repair. *Biomacromolecules* **2017,** *18* (12), 4075-4083.

3 Ulery, B. D.; Nair, L. S.; Laurencin, C. T., Biomedical Applications of Biodegradable Polymers. *Journal of polymer science. Part B, Polymer physics* **2011,** *49* (12), 832-864.

4 Schubert, R. Fracture healing | Radiology Reference Article. https://radiopaedia.org/articles/fracture-healing?lang=us (accessed Mar 29, 2019).

5 Jahandideh, A.; Muthukumarappan, K., Star-shaped lactic acid based systems and their thermosetting resins; synthesis, characterization, potential opportunities and drawbacks. *European Polymer Journal* **2017,** *87*, 360-379.

6 Breitenbach, A.; Li, Y. X.; Kissel, T., Branched biodegradable polyesters for parenteral drug delivery systems. *Journal of Controlled Release* **2000,** *64* (1), 167-178.

7 Kwee, T.; Taylor, S. J.; Mauritz, K. A.; Storey, R. F., Morphology and mechanical and dynamic mechanical properties of linear and star poly(styrene-b-isobutylene-b-styrene) block copolymers. *Polymer* **2005,** *46* (12), 4480-4491.

8 Theodorakis, P. E.; Avgeropoulos, A.; Freire, J. J.; Kosmas, M.; Vlahos, C., Effects of the Chain Architecture on the Miscibility of Symmetric Linear/Linear and Star/Star Polymer Blends. *Macromolecules* **2006,** *39* (12), 4235-4239.

9 Pitt, C. G.; Chasalow, F.; Hibionada, Y.; Klimas, D.; Schindler, A. Aliphatic polyesters. I. The degradation of poly (ϵ-caprolactone) in vivo. J. Appl. Polym. Sci. **1981**, 26 (11), 3779−3787.

10 Woodard, L. N.; Page, V. M.; Kmetz, K. T.; Grunlan, M. A., PCL–PLLA Semi-IPN Shape Memory Polymers (SMPs): Degradation and Mechanical Properties. *Macromolecular Rapid Communications* **2016,** *37* (23), 1972-1977.

11 Woodard, L. N.; Grunlan, M. A., Hydrolytic Degradation and Erosion of Polyester Biomaterials. *ACS Macro Letters* **2018,** *7* (8), 976-982.

12 Gong, J. P., Why are double network hydrogels so tough? *Soft Matter* **2010,** *6* (12), 2583-2590.

13 Yoshikawa, H.; Tamai, N.; Murase, T.; Myoui, A., Interconnected porous hydroxyapatite ceramics for bone tissue engineering. *Journal of the Royal Society, Interface* **2009,** *6 Suppl 3* (Suppl 3), S341-S348.

14 Zhang, D.; George, O. J.; Petersen, K. M.; Jimenez-Vergara, A. C.; Hahn, M. S.; Grunlan, M. A., A bioactive "self-fitting" shape memory polymer scaffold with potential to treat cranio-maxillo facial bone defects. *Acta Biomaterialia* **2014,** *10* (11), 4597-4605.

15 Tsuji, H.; Ikada, Y., Blends of aliphatic polyesters. II. Hydrolysis of solution-cast blends from poly(L-lactide) and poly(E-caprolactone) in phosphate-buffered solution. *Journal of Applied Polymer Science* **1998,** *67* (3), 405-415.

16 Burke, J.; Donno, R.; d'Arcy, R.; Cartmell, S.; Tirelli, N., The Effect of Branching (Star Architecture) on Poly(d,l-lactide) (PDLLA) Degradation and Drug Delivery. *Biomacromolecules* **2017,** *18* (3), 728-739.

17 Nail, L. N.; Zhang, D.; Reinhard, J. L.; Grunlan, M. A., Fabrication of a Bioactive, PCL-based "Self-fitting" Shape Memory Polymer Scaffold. *Journal of Visualized Experiments* **2015**, No. 104.

18 Wu, W.; Wang, W.; Li, J., Star polymers: Advances in biomedical applications. *Progress in Polymer Science* **2015,** *46*, 55-85.

19 Mahadev Patil, R.; Ghanwat, A. A.; Ganugapati, S.; Gnaneshwar, R., Synthesis and Characterization of Four-Arm Star Poly(ϵ-caprolactone)-Block-Poly(cyclic-carbonate methacrylate) Copolymers by Combining Ring-Opening Polymerization With Atom Transfer Radical Polymerization. *Journal of Macromolecular Science, Part A* **2015,** *52* (2), 114-123.

20 García-Olaiz, G. D.; Montoya-Villegas, K. A.; Licea-Claverie, A.; Cortez-Lemus, N. A., Synthesis and characterization of four- and six-arm star-shaped poly(ε-caprolactone)-b-poly(N-vinylcaprolactam): Micellar and core degradation studies. *Reactive and Functional Polymers* **2015,** *88*, 16-23.

APPENDIX

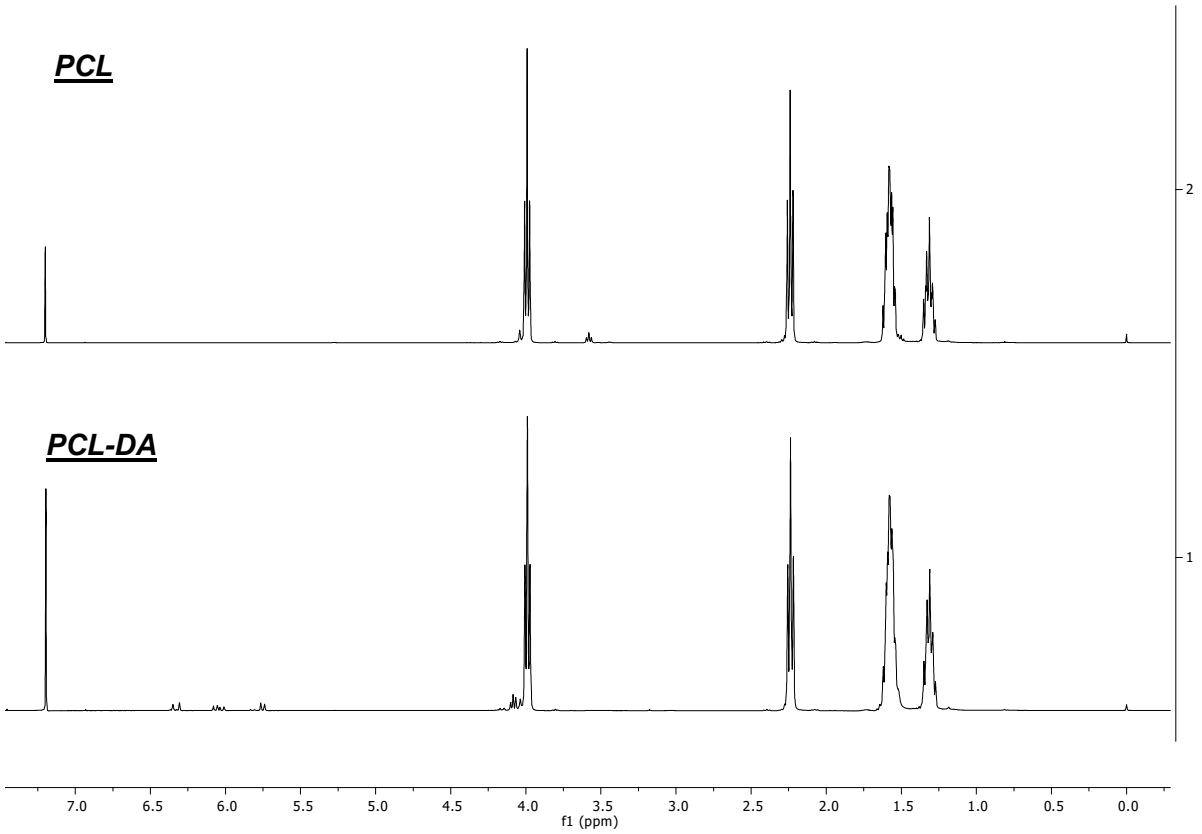

Figure A1. NMR of PCL and PCL-DA (M_n = 10 kg/mol)

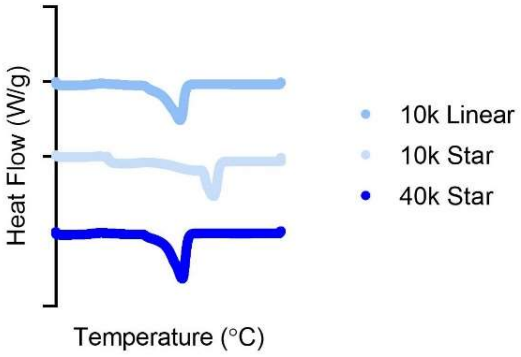

Figure A2. DSC of each PCL polymer.

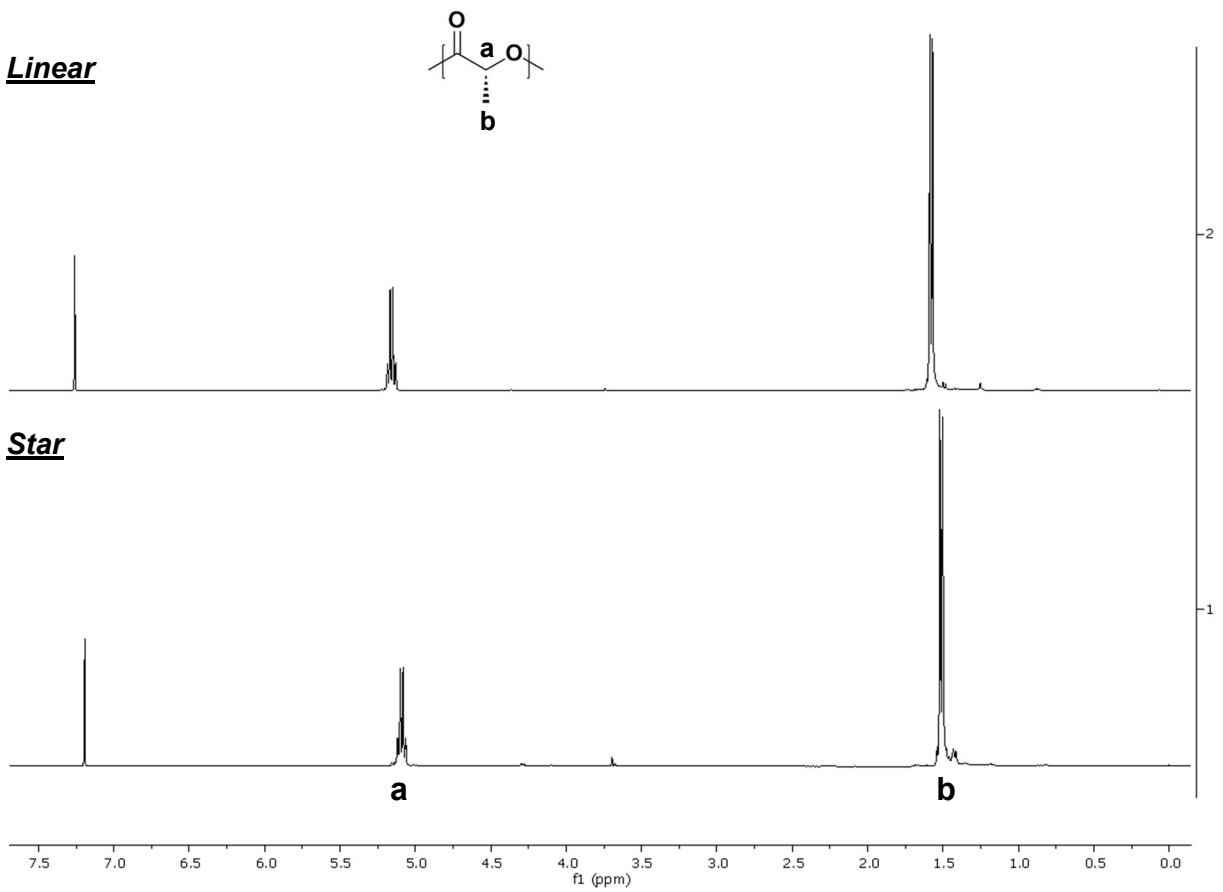

Figure A3. NMR of linear and star PLLA (M_n = 15 kg/mol)

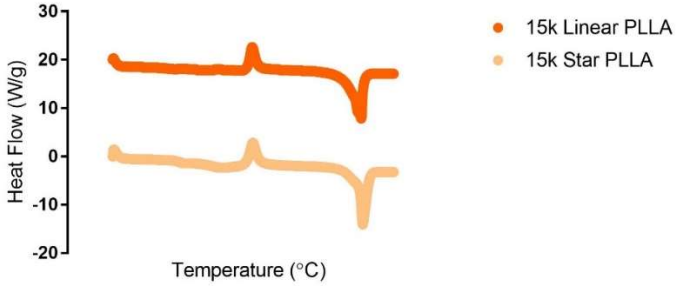

Figure A4. DSC of linear and star PLLA polymers.

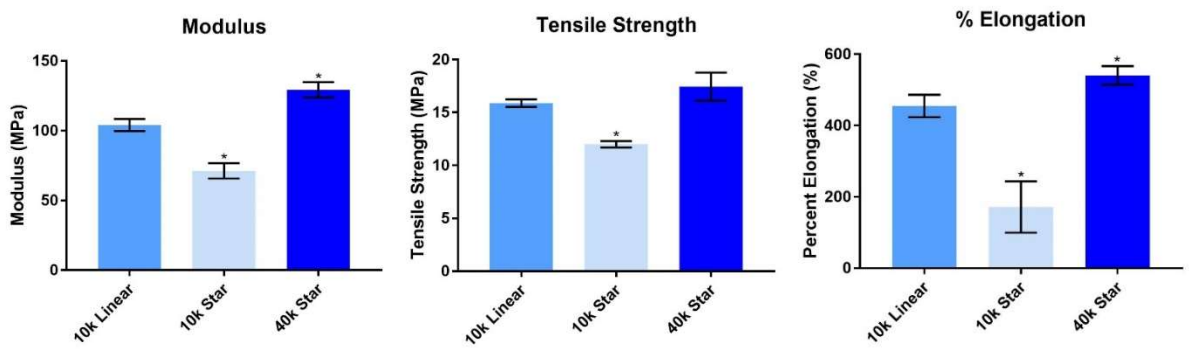

Figure A5. Mechanical properties of different molecular weight PCL-TAs compared to linear PCL-DA.

The tensile modulus (*E*) and tensile strength (TS) were determined for all three PCL networks. Compared to 10k PCL-DA, 40k PCL-TA proved to have a significantly higher modulus of 129 ± 5.5 MPa. The TS of 40k PCL-TA was not significantly different to the control, as it was maintained at 17.6 ± 1.6 MPa.

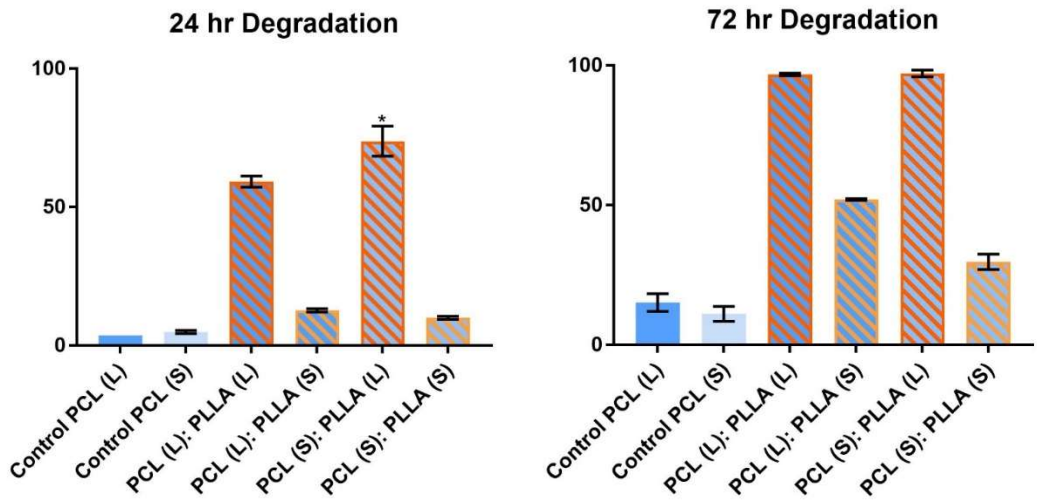

Figure A6. Mass loss at 24 and 72 hours of degradation.

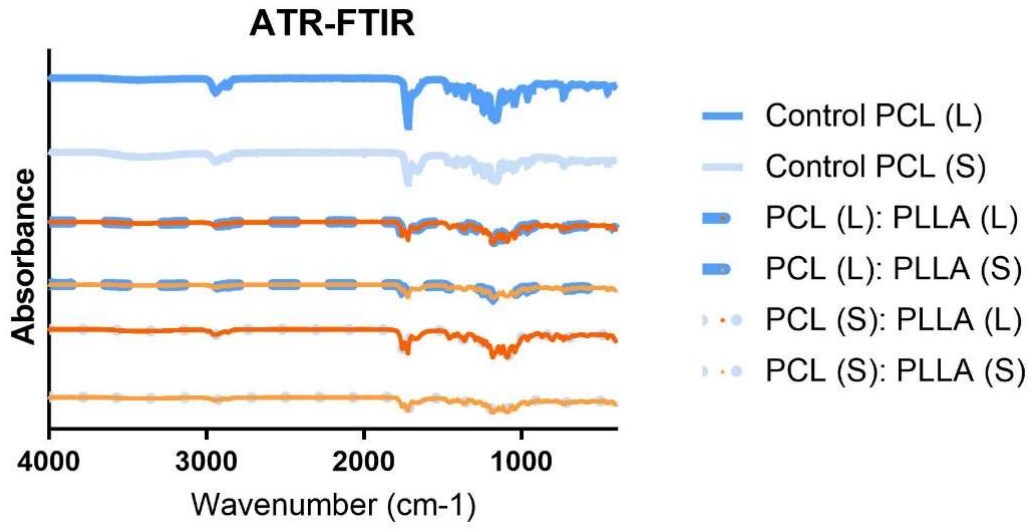

Figure A7. ATR-FTIR of all compositions.

ATR-FTIR was performed on the non-degraded films to quantify the polymer on the surface. The peaks are due to the PCL and PLLA carbonyl bonds having distinct signals; the PCL peak is ~1720 cm^{-1}, and the PLLA peak is ~1760 cm^{-1}. There is less PLLA at the surface of semi-IPNs comprised of star PLLA compared to linear PLLA compositions. This trend is similar to the degradation rates found, as more PLLA on the surface would accelerate the degradation of the film because PLLA degrades faster than PCL.